Proton NMR and μSR in $Mn_{12}O_{12}$ acetate: A mesoscopic magnetic molecular cluster

A. Lascialfari and D. Gatteschi
Department of Chemistry, University of Florence, Firenze, Italy

F. Borsa
Ames Laboratory and Department of Physics and Astronomy, Iowa State University, Ames, Iowa 50011 and Department of Physics ''A. Volta,'' Unita' INFM di Pavia, Via Bassi 6, I27100 Pavia, Italy

A. Shastri and Z. H. Jang
Ames Laboratory and Department of Physics and Astronomy, Iowa State University, Ames, Iowa 50011

P. Carretta
Department of Physics ''A. Volta,'' Unita' INFN di Pavia, Via Bassi 6, I27100 Pavia, Italy
(Received 22 April 1997)

The spin dynamics of Mn spins in the dodecanuclear manganese cluster of formula $[Mn_{12}O_{12}(CH_3COO)_{16}(H_2O)_4]\cdot 2CH_3\text{-}COOH\cdot 4H_2O(Mn_{12})$ has been investigated by ^{1}H NMR and muon spin-lattice relaxation rate $1/T_1$ as a function of temperature (10–400 K) and external magnetic field (0–9.4 T). At room temperature, the proton $1/T_1$ depends on the measuring frequency. The results can be interpreted in terms of a slow decay of the Mn electronic-spin autocorrelation function, a feature characteristic of the almost zero dimensionality of the system. As the temperature is lowered, $1/T_1$ displays a critical enhancement that can be related to the slowing down of the local spin fluctuations as the cluster approaches the condensation into the total spin $S=10$ ground-state configuration. It is found that the application of an external magnetic field greatly depresses the enhancement of $1/T_1$ an effect that could be related to the superparamagnetic behavior of the Mn_{12} molecule. [S0163-1829(98)06801-5]

I. INTRODUCTION

The recent successes in synthesizing solid lattices of weakly coupled molecular building blocks containing strongly interacting spins has opened up the possibility of studying experimentally magnetism at the mesoscopic scale.[1] Each building block in the solid is an identical magnetic cluster and since the magnetic properties are dominated by the intramolecular interactions one has access to the study of the mesoscopic properties even by using techniques that require bulk macroscopic quantities of material. The magnetism of molecular size clusters are of great interest, first, because of the possibility of their providing new useful applications, and second, because of the very basic questions that they pose concerning magnetic properties of ultrasmall complexes.[2]

Molecular clusters containing 6 and 10 iron (III) spins ($S=\frac{5}{2}$) in an almost coplanar ring configuration have been recently investigated by magnetic susceptibility[3,4] and proton NMR.[5] These rings show interesting magnetic and spin dynamical properties associated with the nonmagnetic singlet ground state. On the other hand, the transition-metal acetate complex containing 12 Mn ions, Mn_{12}, form a magnetic cluster with a high total spin ($S=10$) ground-state configuration.[6] The high spin state combined with a large easy-axis anisotropy leads to superparamagnetic behavior at low temperature[7,8] with very slow relaxation of the magnetization that was recently explained in terms of macroscopic quantum tunneling effects.[9]

The crystal structure of Mn_{12} acetate, the Mn valence, and the exchange interactions have been established:[6] the molecular cluster is made up of four tetrahedrally coordinated Mn(IV) ions with $S=\frac{3}{2}$ at the center and eight Mn(III) ions with $S=2$ on the outside. The low-temperature magnetic properties were explained by assuming four different antiferromagnetic exchange coupling constants J. The ground-state configuration is determined by the relative strength of the J constants whereby spin frustration plays an important role in determining the low-temperature spin configuration with the four inner Mn(IV) parallel to each other, the outer eight Mn(III) also parallel and the two groups antiparallel to each other for a total spin value $S=10$. The orbital angular momentum is quenched by the crystal field. However, off-diagonal elements of the spin-orbit interaction generate an effective single-ion anisotropy of Ising type with the tetragonal axis of the crystal as the easy axis.[10] The interactions between the spins of different molecular groups in the crystal are of dipolar nature and thus negligible as indicated by the very small paramagnetic Curie temperature [50 ± 20 mK (Ref. 11)]. With this much known about the molecular cluster one can now model the system and compare experimental results both on the dynamic and the static properties over a wide temperature and magnetic-field range with analytical and/or numerical calculations.

The spin dynamics of the cluster is investigated here by measurements of nuclear spin-lattice relaxation rate T_1^{-1} of both the protons (NMR) and of the muons (μSR) as a function of temperature (4.2–400 K) and of applied magnetic field (0–9.1 T). In both cases the relaxation rate is determined by the fluctuation spectrum of the local field at the

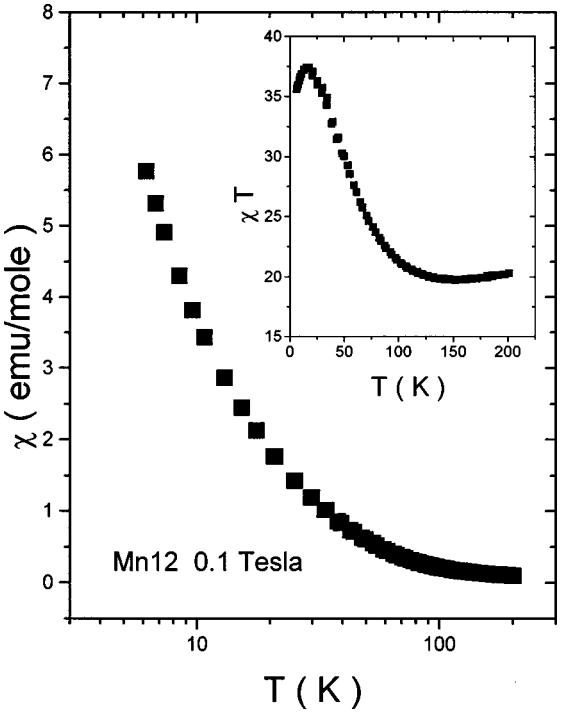

FIG. 1. dc magnetic susceptibility in Mn_{12} plotted as a function of temperature for a magnetic field of 0.1 T. In the inset the effective Curie constant χT is plotted vs T.

nuclear (muon) site generated by the hyperfine interaction with the localized Mn magnetic moments. The static properties are established by the magnetization measurements as a function of temperature for different applied magnetic fields.

II. EXPERIMENTAL RESULTS

The measurements were performed on a polycrystalline sample of the dodecanuclear manganese cluster of formula $[Mn_{12}O_{12}(CH_3COO)_{16}(H_2O)_4]\cdot 2CH_3\text{-}COOH\cdot 4H_2O$ that has an overall D_{2d} symmetry.[6] The manganese (III) ions define an external octagon, whereas the manganese (IV) ions correspond to an internal tetrahedron. In the crystal lattice all the molecules have the S_4 symmetry axis parallel to the crystallographic c axis and the shortest intercluster contacts between metal ions are larger than 7 Å. As previously mentioned, we can consider the ground state as having all the manganese (III) spins of a cluster up and the manganese (IV) spins down, resulting in a total spin $S=10$.

Measurements of dc magnetic susceptibility were performed at 0.1 T by using a Metronique Ingegnerie superconducting quantum interference device susceptometer operating in the range 3–280 K. In the applied magnetic fields, with lowering temperature the powders tend to reorient themselves thus giving susceptibility data not corresponding to a random powder distribution. Furthermore at low temperature a saturation effect in the susceptibility values is present. This circumstance explains the difference obtained in our present dc susceptibility data at 0.1 T when compared with previously published[6] data (ac measurements in zero field and dc measurements at 1 T). The results are shown in Fig. 1.

^{1}H pulsed NMR experiments were performed with three different kinds of pulse Fourier transform (FT) spectrometers at the University of Florence, at Iowa State University, and at the University of Pavia. The powders were pressed in order to avoid the (re)orientation of the grains. The $\pi/2$ pulse length was comprised between 1 μs and 10 μs depending on the type of spectrometer and on the operating frequency. In most cases the radiofrequency field H_1 was sufficiently strong to irradiate the whole NMR line. The exceptions were at the maximum field (9.1 T) and at low temperatures ($T<40$ K). Whenever the whole line could be irradiated with one radio frequency pulse the NMR spectra were obtained with identical results either from the FT of the free precession decay or from the FT of the half echo signal. The broad spectrum at low temperature was obtained by plotting the echo intensity at different values of the irradiation frequency. The spin-lattice relaxation rates were measured with the inversion recovery method at $T>130$ K and with the saturation recovery pulse sequence at low temperatures. Deviations from an exponential recovery of the nuclear magnetization were observed only in the high field ($H>2$ T) and low-temperature ($T<100$ K) measurements when the NMR spectrum becomes broader than about 200 KHz [see Fig. 2(a)].

Since there are 56 protons in each molecular cluster with many different hyperfine couplings to the Mn magnetic moments, the NMR powder spectrum is inhomogeneously broadened by the distribution of paramagnetic shifts. Thus its width increases with increasing magnetic field and its shape shows some asymmetry. Also one expects a multiplicity of relaxation rates. However, the spin-spin relaxation time T_2 is very fast (20–40 μs) and thus in most of the measurements a common spin temperature is achieved by the nuclei during the recovery, yielding an exponential function with a time constant representing the average relaxation rate. When the recovery was nonexponential we measured the initial slope of the recovery curve that is approximately equal to the tangent at the origin of time. The procedure is illustrated in Fig. 2(a). The parameter obtained from the initial recovery measures an average relaxation rate. In conclusion, the measured parameter T_1^{-1} represents in all cases the weighted average of the relaxation rates of the nonequivalent protons in the cluster. Details of this analysis can be found in Ref. 5.

The dependence of the nuclear spin-lattice relaxation rate on the external magnetic field at room temperature is shown in Fig. 3. The enhancement of T_1^{-1} at low fields is similar to what is observed in one-dimensional paramagnetic chains[12,13] and is quite in contrast with the field independence normally observed in three-dimensional insulating paramagnets well above the ordering temperature.[14]

The temperature dependence of T_1^{-1} at different values of the applied magnetic field is shown in Fig. 4. On lowering the temperature the relaxation rate increases dramatically and, except for the high-field data, the signal becomes unobservable (the spin-spin relaxation time T_2, not shown in Fig. 4, becomes also very short). At very low temperatures, T_1 and T_2 resume values sufficiently long to allow for the measurements to be performed. However, it is noted that below 30 K the NMR spectrum becomes very broad (of the order of 1 Mhz in 4.6 T field) and thus the T_1^{-1} parameter is affected by a large experimental uncertainty.

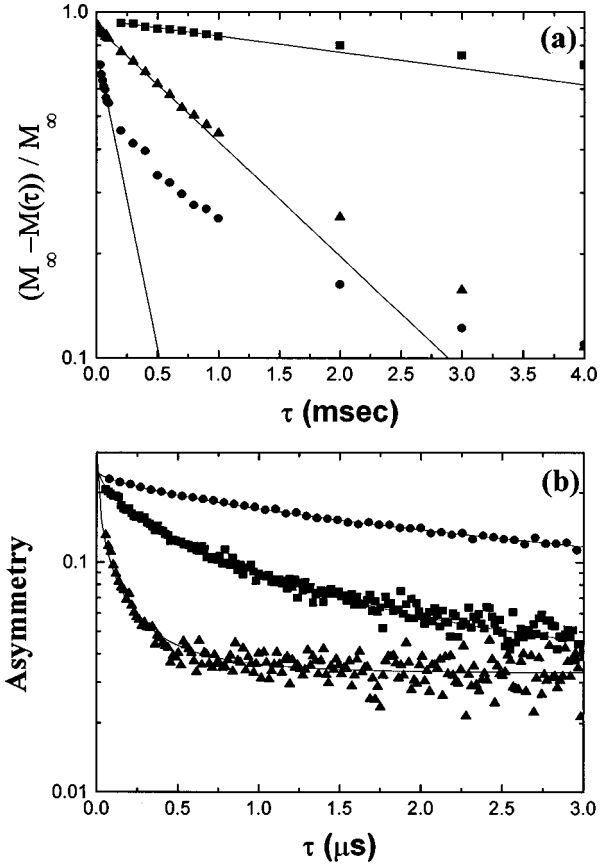

FIG. 2. (a) Semilog plot of the recovery of the nuclear magnetization as a function of the time interval between the saturation pulse sequence and the signal. The curves shown refer to proton NMR in Mn_{12} at resonance frequency of 87 MHz for three different temperatures: (▲) $T=300$ K; (●) $T=43$ K; (■) $T=4.2$ K. The straight lines represent the slope of the tangent at the origin that defines the measured average T_1^{-1} (see text). (b) Semilog plot of the decay of the muon polarization in longitudinal field ($H=1040$ G) for three different temperatures in Mn_{12}: (●) $T=60$ K; (■) $T=40$ K; (▲) $T=14$ K. The solid lines show the best fit according to a stretched exponential behavior (see text).

μ^+SR measurements were performed at ISIS pulsed muon facility (Rutherford Appleton Laboratory) on MUSR beam line. The measurements were carried out either in zero field (ZF) or in a longitudinal field (LF) $H=1040$ G using a statistic of about 15 million events. In the LF experiments the decay of the muon polarization was characterized by a stretched exponential behavior $\{\exp[-(\lambda t)^{\beta}]\}$ with an initial asymmetry around $A=0.22$ plus a constant background $A=0.02$ associated with muons stopping in the sample holder [see Fig. 2(b)]. The stretched exponential behavior indicates a distribution of muons sites and the exponent β is observed to decrease from 0.75 to 0.6 in the temperature range 20 K $<T<100$ K, while a faster decrease is observed below 20 K. In ZF the decay is also characterized by a Gaussian component originating from the dipolar interaction of the muons with the surrounding nuclei. The component is quenched in the LF of 1040 G.

The temperature dependence of λ in zero field and in presence of an applied magnetic field is shown in Fig. 5. A magnetic field of 1040 G corresponds for muons ($\gamma=135.5$ MHz/T) to a nuclear Larmor resonance frequency of 14.1 MHz. In the inset of Fig. 5 we compare the muon relaxation rate with the proton relaxation rate for the same measuring frequency. Apart from a rescaling factor due to the different hyperfine coupling of the two probes the two sets of data

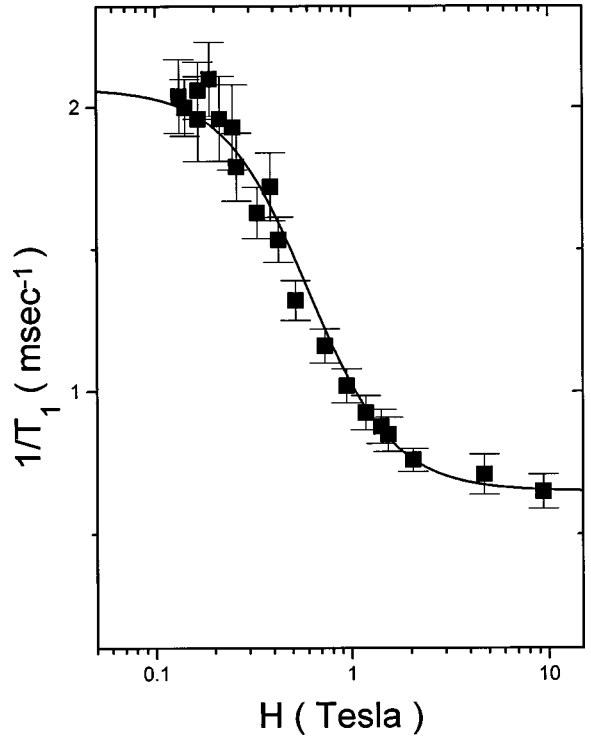

FIG. 3. ^{1}H nuclear spin-lattice relaxation rate as a function of external magnetic field at room temperature in Mn_{12}. The line corresponds to the fit according to Eq. (6).

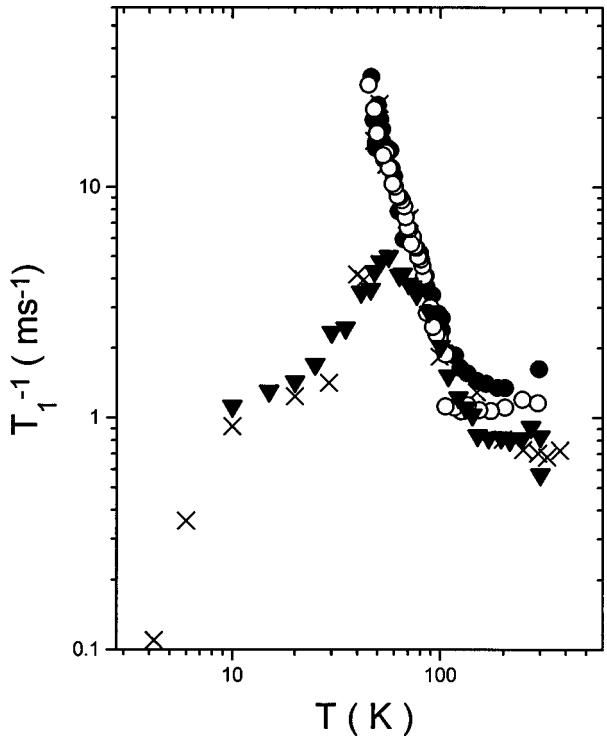

FIG. 4. ^{1}H nuclear spin-lattice relaxation rate in Mn_{12} vs temperature: (●) 14.1 MHz. (○) 31 MHz; (×) 87 MHz; (▼) 200 MHz.

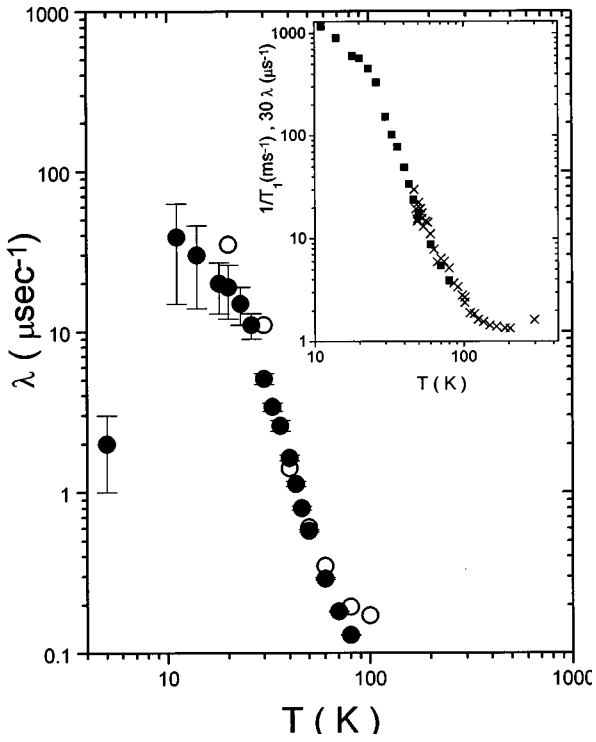

FIG. 5. Muon longitudinal relaxation rate in Mn_{12} plotted as a function of temperature: (○) zero field; (●) 0.1 T. In the inset we compare the relaxation rate of the protons (×) with one of the muons (■). The data for the protons are at 14.1 MHz which corresponds to the Larmor frequency of the muons in the external field of 0.1 T. By rescaling one set of data the two sets overlap in a wide temperature region.

overlap over a wide temperature region. This is a strong indication that in both cases the relaxation rate is driven by the Mn spin dynamics and that the details of the hyperfine coupling of the different protons to the Mn spins is not important in determining the overall temperature dependence of the spin dynamics.

III. DISCUSSION

The general expression for the spin-lattice relaxation rate due to the coupling of the protons to the fluctuating Mn spins is[13,14]

$$1/T1=(\hbar\gamma_n\gamma_e)^2/(4\pi g^2\mu_B^2)k_BT\left[\tfrac{1}{4}\sum_q A^{\pm}(q)\chi^{\pm}(q)f_q^{\pm}(\omega_e)+\sum_q A^z(q)\chi^z(q)f_q^z(\omega_n)\right], \quad (1)$$

where γ_n and γ_e are the gyromagnetic ratios of the nucleus and of the free electron, respectively, g is the Lande' factor, μ_B is the Bohr magneton, k_B is the Boltzmann constant. The coefficients $A^{\pm}(q)$ and $A^z(q)$ are the Fourier transforms of the spherical components of the product of two dipole-interaction tensors[13] describing the hyperfine coupling of a given proton to the Mn magnetic moments whereby the symbols $\pm$ and z refer to the components of the Mn spins transverse and longitudinal with respect to the quantization direction that is here the external magnetic field. In order to obtain Eq. (1) the collective q-dependent spin-correlation function of the Mn, i.e., $\langle S(q,t)S(q,0)\rangle$, is written as the product of the static response function times a normalized relaxation function $f_q^{\pm,z}(t)$.

A. Magnetic-field dependence of the nuclear relaxation at room temperature

The theoretical evaluation of the relaxation rate from Eq. (1) requires three steps. First one must compute the geometrical coefficients $A^{\pm,z}(q)$. This can be done in principle assuming a purely dipolar interaction between the nuclei and the Mn moments and from the knowledge of the intramolecular distances and angles. In practice, the result will not be very sensitive to details of the molecular structure since one has to take averages over many proton sites and over an isotropic distribution of orientations of the molecule with respect to the external applied field.[13] The second step is to solve for the thermodynamic equilibrium properties of the Mn_{12} cluster, i.e., to obtain an expression for the wave-vector-dependent susceptibility $\chi(q,T)$. Exact analytical results have been derived for the one-dimensional classical Heisenberg model both for free[15] and for cyclic boundary conditions[16] and have been applied to explain the uniform magnetic susceptibility of simple coplanar rings of iron (III) ions.[17] On the other hand, the Mn_{12} cluster has a complicated structure with four different antiferromagnetic nearest-neighbor coupling constants leading to spin frustration and no exact solutions are yet available even for the classical Heisenberg approximation. The third and most difficult step is the evaluation of the spin dynamics that requires the calculation of the decay in time of the spin-correlation function (CF). An approximate expression for the CF can be obtained for an infinite Heisenberg classical chain at high temperature by matching the short-time expansion to the long-time diffusive behavior due to the conservation of the total spin operator.[12] For temperatures $T\gg J/k$ the conservation property can be incorporated for spins on a ring by means of a discretized diffusion equation to which cyclic boundary conditions are applied. For this model it is found[18] that the autocorrelation function decays rapidly at short times until it reaches a constant value that depends on the number of spins in the cluster. The plateau in the CF is reached after a time of the order of $10\omega_D^{-1}$ where ω_D is the exchange frequency given, at the simplest level of approximation, by

$$\omega_D=Da_0^{-2}=(2\pi J/h)[S(S+1)]^{1/2}, \quad (2)$$

with J the exchange constant between nearest-neighbor spins S. A qualitatively similar result is obtained for the CF by using a one-dimensional hopping model on a closed loop.[19] The leveling off of the time dependence of the CF at a value $1/N$ with N the number of spins in the cluster is the result of the conservation of the total spin component for an isotropic spin-spin interaction. In practice, the anisotropic terms in the spin Hamiltonian will produce a decay of the CF via energy exchange with the ''lattice.'' A sketch of the time decay of the CF and of the corresponding spectral density is shown in Fig. 6. The decay at long time of the CF has a cutoff at a time Γ_A^{-1} due to the anisotropic terms in the spin Hamiltonian.[20] In the following we will discuss the

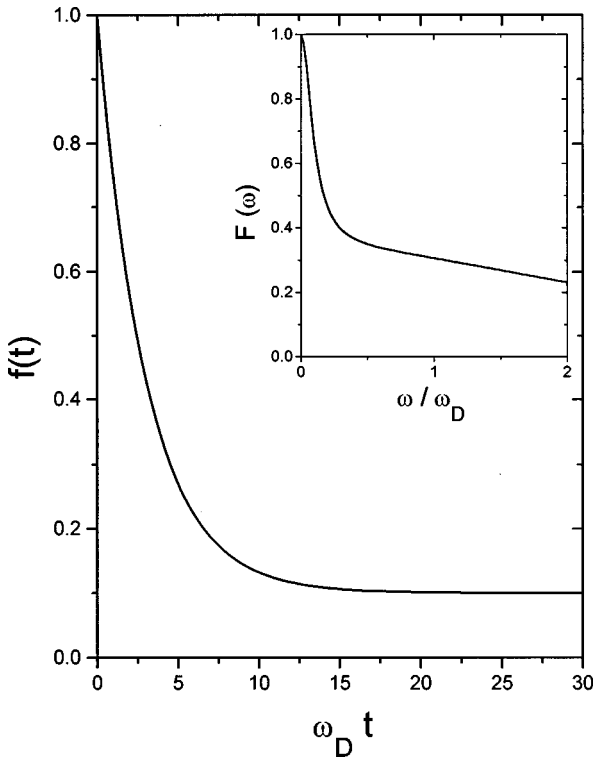

FIG. 6. Sketch of the decay in time of the autocorrelation function of the Mn spin. The initial fast decay is characterized by the constant Γ_D^{-1} while the slow decay at long time is characterized by the constant Γ_A^{-1} (see text). The inset shows the corresponding Fourier transform or spectral density function.

magnetic-field dependence of the nuclear relaxation rate at room temperature in terms of a simplified model that incorporates the theoretical understanding of the spin dynamics in clusters as described above.

From the investigation of the magnetochemical properties of Mn_{12} it was concluded[6] that the Mn spins in the cluster are coupled by four different antiferromagnetic nearest-neighbors exchange parameter whereby only the one that couples four Mn spins of the outer shell to the four spins of the inner shell is larger than room temperature, i.e., $J/k > 300$ K. Thus we expect that most of the correlation effects leading to the high spin ground state $S=10$ will develop below room temperature and we assume in the following a high-temperature approximation to analyze the magnetic-field dependence of the relaxation rate at room temperature. We neglect in Eq. (1) the q-dependence of the generalized susceptibility $\chi^{\alpha}(q)$, and of the spectral density function $f_q^{\alpha}(\omega)$. We assume an isotropic response function $\frac{1}{2}\chi^{\pm}(q) = \chi^{z}(q) = \chi(q=0)$ and we take a q-independent average value for the dipolar hyperfine interaction of the protons with the local moment of the Mn spins: $A^{\pm}(q) = A^{\perp}$; $A^{z}(q) = A^{z}$ in units of cm^{-6}. Then Eq. (1) reduces in this high-temperature limit to

$$1/T_1 = (\hbar\gamma_n\gamma_e)^2/(4\pi g^2\mu_B^2) k_B T \chi(q=0)[\tfrac{1}{2}A^{\pm}\Phi^{\pm}(\omega_e) + A^{z}\Phi^{z}(\omega_n)], \tag{3}$$

where $\Phi^{\alpha}(\omega) = \Sigma_q f_q^{\alpha}(\omega)$ are the Fourier transforms of the autocorrelation functions of the transverse ($\alpha = \pm$) and longitudinal ($\alpha = z$) components, respectively, of the local Mn spin, ω_n and ω_e are the Larmor frequencies of the proton and of the free electron, respectively. Furthermore, on the basis of the time dependence of the CF discussed above and sketched in Fig. 6, we model the spectral function in Eq. (3) as the sum of two components:

$$\Phi^{\pm}(\omega) = \Phi^{z}(\omega) = \Phi'(\omega) + \Gamma_A/(\omega^2 + \Gamma_A^2), \tag{4}$$

where we assume the same CF for the decay of the transverse ($\pm$) and longitudinal (z) components of the Mn spins. The first term in Eq. (4) represents the Fourier transform of the initial fast decay of the CF while the second term represents the FT of the decay at long time of the CF due to anisotropic terms in the spin Hamiltonian and we model this second part with a Lorenzian function of width Γ_A.

From Eq. (2) one can estimate a diffusion frequency $\omega_D \approx 10^{14}$ Hz for $J/k = 200$ K and $S=2$ or $S=\frac{3}{2}$. The spectral function $\Phi'(\omega)$ reaches a plateau and becomes almost frequency-independent for $\omega < \omega_D/10$ (Refs. 18 and 19) (see also Fig. 6). For the magnetic-field strength used in the experiment (see Fig. 2) both ω_n and ω_e are smaller than $\omega_D/10$. Thus we will assume $\Phi'(\omega_n) = \Phi'(\omega_e) = \Gamma_D^{-1}$ in Eq. (3) where the characteristic frequency Γ_D is of the same order of magnitude as $\omega_D/10$. Finally, by assuming $\omega_n \ll \Gamma_A$ in Eq. (4), Eq. (3) can be rewritten as

$$1/T_1 = (\hbar\gamma_n\gamma_e)^2/(4\pi g^2\mu_B^2) k_B T \chi(q=0)[\tfrac{1}{2}A^{\pm}\Gamma_A/(\omega_e^2 + \Gamma_A^2) + \tfrac{1}{2}A^{\pm}/\Gamma_D + A^{z}(1/\Gamma_D + 1/\Gamma_A)]. \tag{5}$$

The experimental data in Fig. 3 were fitted by using an expression of the form of Eq. (5). The result is

$$1/T1 = 0.57/(0.36 + H^2) + 0.55 \quad (\mathrm{msec}^{-1}), \tag{6}$$

where the magnetic field H is expressed in Tesla.

The width Γ_A of the narrow component in the spectral function represents the frequency that characterizes the exponential time decay of the spin CF in the cluster due to anisotropic terms in the spin Hamiltonian. By comparing Eq. (5) with the numerical fit [Eq. (6)] with $(\hbar\gamma_n\gamma_e)^2/(4\pi) = 1.94\times10^{-32}$ $(\mathrm{sec}^{-2}\mathrm{cm}^{6})$ and assuming $k_B T\chi(q=0)/g^2\mu_B^2 = 1$, one has $\Gamma_A/\gamma_e = 0.6$ T corresponding to $\Gamma_A = 10^{11}\ \mathrm{sec}^{-1}$ or $\hbar\Gamma_A/k_B = 0.8$ K. This value is consistent with the single-ion anisotropy in the Mn_{12} cluster deduced from the low-temperature magnetic properties, i.e., $D = 0.75$ K.[6] Also one deduces $A^{\pm} = 1.5\times10^{46}\ \mathrm{cm}^{-6}$. Since $A^{\pm}$ is the product of two dipolar interaction tensor components, it is of order of r^{-6} where r is the distance between a ^{1}H nucleus and a Mn local moment. The value obtained from the fit corresponds to $r = 2$ Å which, although shorter than expected for the average proton-manganese distance,[21] can be considered acceptable given the simplicity of the model used. Also, by comparing Eq. (5) with the numerical fit [Eq. (6)] and using $\Gamma_D = 10^{13}\ \mathrm{sec}^{-1}$, one obtains $A^{z} = 3.35\ 10^{45}\ \mathrm{cm}^{-6} = 0.22\ A^{\pm}$.

B. Temperature dependence of the nuclear relaxation rate

As seen in Fig. 4, the relaxation rate is characterized by a weak temperature dependence in the interval 100–300 K and by a rapid increase of the relaxation rate as T decreases

below 100 K followed by a maximum that depends on the applied magnetic field. It is noted that the enhancement of $1/T_1$ starting below 100 K appears to be correlated with the increase of the effective Curie constant $C_{\rm eff}=\chi T$, as shown in Fig. 1.

The effective Curie constant in Fig. 1 increases by a factor of almost 2 as T decreases from 100 to 20 K. If $C_{\rm eff}$ is assumed to be proportional to the square of the effective magnetic moment of the Mn_{12} molecule, then one finds that at high temperature, where the Mn spins can be assumed to be uncorrelated, $C_{\rm eff}\propto 8s_1(s_1+1)+4s_2(s_2+1)=63$ where we take $s_1=2$ for the 8 outer Mn spins and $s_2=\frac{3}{2}$ for the 4 inner Mn spins.[6] At low temperature where the cluster is in its ground state with total spin $S=10$, one expects $C_{\rm eff}\propto S(S+1)=110$ that corresponds indeed to an increase by a factor of 2. Thus the critical enhancement of the relaxation rate at low temperature should be related to the increase of the correlation among Mn moments with the consequent slowing down of the fluctuations.

A theoretical description of the relaxation rate will start from Eq. (1) and it requires the calculation of the static q-dependent response function $\chi(q)$ and of the spectral density function $f(q,\omega)$. This calculation is underway[18] by using a semiclassical treatment of the interacting Mn moments. The results should describe the spin dynamics as the system approaches the temperature of condensation into the $S=10$ ground state in a way similar to the approach to the magnetic transition temperature for a thermodynamic system.

In view of the experimental character of the present investigation, we limit ourselves to give a qualitative interpretation of the T_1^{-1} results in terms of a phenomenological description of the critical slowing down of the fluctuations whereby one expects that T_1^{-1} should diverge at low temperature with some power-law dependence of the type $T_1^{-1}\propto(T-T_N)^{-n}$ where for a one-dimensional system with no long-range order $T_N=0$.[13] By maintaining the same approximations that led to Eq. (5), we show in the following that we can incorporate the critical temperature dependence of the parameters in Eq. (6) in a phenomenological way that leads to a semiquantitative explanation of the experimental data. Since the parameter Γ_A represents the frequency of exchange of energy of the Mn spins with the lattice due to the single-ion anisotropy in the spin Hamiltonian, it should not depend on the intracluster spin correlations and it will thus be assumed to be temperature-independent. On the other hand, the parameter Γ_D that describes the decay of the CF due to the nearest-neighbor exchange coupling J between Mn spins, should decrease as the intracluster spin correlations increase. We assume $\Gamma_D\propto T^n$ in analogy with what is found in the one-dimensional antiferromagnetic Mn chain TMMC $[(CH_3)_4NMnCl_3]$.[13] Finally we incorporate the temperature dependence of the uniform spin susceptibility by using the experimental results in Fig. 1. Therefore the expression for the relaxation rate becomes:

$$1/T_1=[1/T_{10}(H)+2.1\times10^{11}/\Gamma_D(T)]\chi(T)/\chi(200\ \text{K})\quad(\text{msec}^{-1}),\quad(7)$$

where $1/T_{10}(H)$ is the field dependent room temperature value given by Eq. (6). Note that we set $\chi(T)/\chi(200\,\text{K})=1$ for $T\geqslant 200$ K and that the term containing $\Gamma_D(T)$ is negligible at room temperature. Furthermore we used the same values of the parameters as determined from the field dependence of $1/T_1$, namely, $(\hbar\gamma_n\gamma_c)^2/(\frac{1}{2}\times A^{\pm}+A^z)=2.1\times10^{11}(\text{sec}^{-2})$. In Fig. 7 we show the comparison of the experimental data with the curves obtained from Eq. (7) with $\Gamma_D(T)=1.5\times10^5\times T^3$ and for two values of the external magnetic field. The general behavior of the data at low magnetic field appears to be well represented for a choice of the critical exponent $n=3$ for the temperature dependence of $\Gamma_D(T)$. Also the value of $\Gamma_D(300\,\text{K})=4\times10^{12}$ (rad sec^{-1}) is consistent with the discussion in the previous paragraph about the decay of the CF at room temperature. At high magnetic field one observes a maximum in $1/T_1$ followed by a decrease at low temperature that cannot yet be interpreted. One possibility is that the magnetic field has the effect of quenching the spin fluctuations. The other explanation is that the characteristic frequency Γ_D of the fluctuations reaches the range of either the nuclear or electronic Larmor frequency at the temperature of the maximum. In this second case it is of interest to compare the characteristic frequency of the fluctuations as obtained from NMR and μSR with the ones obtained from the relaxation of the macroscopic magnetization. From ac susceptibility measurements in Mn_{12} it was found[7] that the molecules show superparamagnetic behavior in the temperature range 2–30 K with a relaxation time of the macroscopic magnetization given by an Arrhenius law $\tau=\tau_0\exp(\Delta E/kT)$ with $\tau_0=2.6\times10^{-7}$ sec and $\Delta E/k=64$ K. On the other hand, from the maximum of T_1^{-1}

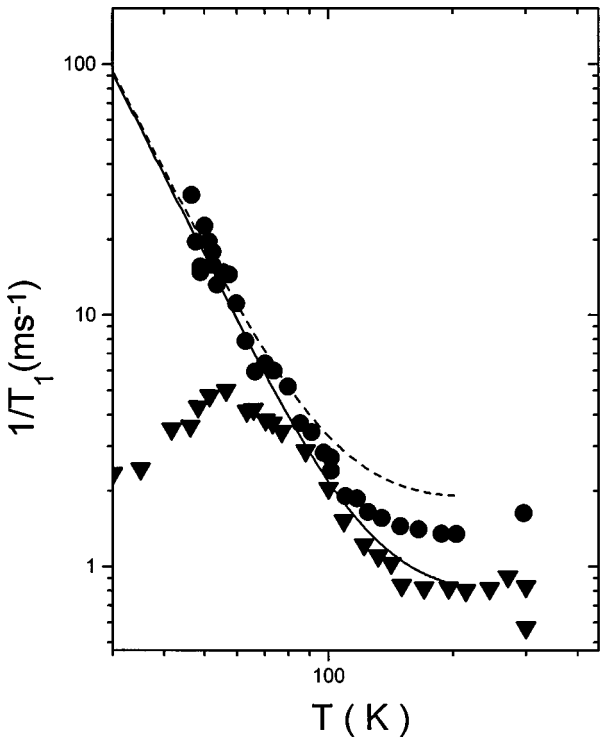

FIG. 7. Plot of the proton relaxation rate in Mn_{12} for the highest frequency 200 MHz (▼), and for the lowest frequency 14.1 MHz (●). The experimental points are the same as in Fig. 4. The full curve and the dashed one are the theoretical curves according to Eq. (7) in the text for the high frequency and for the low frequency, respectively.

in Fig. 4 at $T \approx 60$ K and $\omega_L = 2\pi$ 200 MHz, one has $\tau_{\mathrm{NMR}} = 1/\omega_L = 8 \times 10^{-10}$ sec and from the maximum of λ in Fig. 5 at $T \approx 12$ K and $\omega_\mu = 14$ MHz, one has $\tau_\mu = 1/\omega_\mu = 1.1 \times 10^{-8}$ sec. Both these values are two orders of magnitude faster than the corresponding relaxation time extrapolated from the above Arrhenius law for the macroscopic magnetization. Thus it appears that in order to find an explanation for the maximum of the relaxation rate, systematic measurements at different magnetic fields using different probes such as deuterium nuclei and muons have to be performed and a theoretical understanding of the effects of the magnetic field on the spin excitations in the $S = 10$ ground state has to be achieved.

ACKNOWLEDGMENTS

We thank M. Luban and J. H. Luscombe for helpful discussions and for sharing with us their unpublished theoretical results. This work was supported by funds from Ministero per L'Universita' e la Ricerca Scientifica e Tecnologica, and Consiglio Nazionale delle Ricerche. Ames Laboratory is operated for U.S. Department of Energy by Iowa State University under Contract No. W-7405-Eng-82. This work at Ames Laboratory was supported by the Director for Energy Research, Office of Basic Energy Sciences. The μSR measurements at RAL were carried out under the financial support of the CEE TMR program.

[1] D. Gatteschi, A. Caneschi, L. Pardi, and R. Sassoli, Science **265**, 1055 (1994).
[2] D. D. Awschhalom and D. P. DiVincenzo, Phys. Today **48**, No. 4, 43 (1995), and references therein.
[3] A. Caneschi, A. Cornia, A. C. Fabretti, S. Foner, D. Gatteschi, R. Grandi, and L. Schenetti, Chem. Eur. J. **2**, 1379 (1996).
[4] K. L. Taft, C. D. Delfs, G. C. Papaefthymiou, S. Foner, D. Gatteschi, and S. J. Lippard, J. Am. Chem. Soc. **116**, 823 (1994).
[5] A. Lascialfari, D. Gatteschi, F. Borsa, and A. Cornia, Phys. Rev. B **55**, 14 341 (1997).
[6] R. Sessoli, Hui-Lien Tsai, A. R. Schake, Sheyi Wang, J. B. Vincent, K. Folting, D. Gatteschi, G. Christou, and D. N. Hendrickson, J. Am. Chem. Soc. **115**, 1804 (1993), and references therein.
[7] R. Sessoli, D. Gatteschi, A. Caneschi, and M. A. Novak, Nature (London) **365**, 141 (1993).
[8] J. R. Friedman, M. P. Sarachik, J. Tejada, and R. Ziolo, Phys. Rev. Lett. **76**, 3830 (1996).
[9] P. Politi, A. Rettori, F. Hartmann-Boutron, and J. Villain, Phys. Rev. Lett. **75**, 537 (1995).
[10] Francoise Hartmann-Boutron, Paolo Politi, and Jacques Villain, Int. J. Mod. Phys. B **10**, 2577 (1996).
[11] C. Paulsen *et al.*, J. Magn. Magn. Mater. **140-144**, 379 (1995).
[12] F. Borsa and M. Mali, Phys. Rev. B **9**, 2215 (1974).
[13] D. Hone, C. Sherer, and F. Borsa, Phys. Rev. B **9**, 995 (1974).
[14] T. Moriya, Prog. Theor. Phys. **28**, 371 (1962).
[15] M. E. Fisher, Am. J. Phys. **32**, 343 (1964).
[16] G. S. Joyce, Phys. Rev. **155**, 478 (1967); see also J. H. Luscombe and M. Luban (unpublished).
[17] J. H. Luscombe, M. Luban, and F. Borsa (unpublished).
[18] J. H. Luscombe and M. Luban, J. Phys.: Condens. Matter **9**, 6913 (1997).
[19] J. Tang, S. N. Dikshit, and J. R. Norris, J. Chem. Phys. **103**, 2873 (1995).
[20] J. P. Boucher, M. Ahmed Bakheid, M. Nechschtein, G. Bonera, M. Villa, and F. Borsa, Phys. Rev. **13**, 4098 (1976).
[21] T. Lis, Acta Crystallogr., Sect. B: Struct. Crystallogr. Cryst. Chem. **36**, 2042 (1980).